

Analysis of Double-Layered Finlines Containing a Magnetized Ferrite

MASAHIRO GESHIRO, MEMBER, IEEE, AND TATSUO ITOH, FELLOW, IEEE

Abstract — The characteristics of propagation of the dominant mode in magnetized-ferrite-loaded double-layered finlines are studied. The analysis is based on Galerkin's method applied in the Fourier transform domain. Numerical results are presented for various values of structural and material parameters.

I. INTRODUCTION

RECENTLY, SEVERAL analytical methods for finlines consisting of ferrite have been investigated with a view to applying such waveguides structures to nonreciprocal devices for millimeter-wave integrated-circuit techniques. Beyer *et al.* have reported the analysis of the finline ferrite isolator by the field expansion method based on the TE-mode approximation [1]. More rigorous analyses based on the mode matching method [2], [3] or the spectral-domain method [4], [5] have also been presented. Although some of them claim to be applicable to the analysis of multilayered structures, no extensive results seem to have been published to date. From a practical point of view, multilayered structures should be suitable for integrated circuits.

This paper presents an analysis of ferrite-loaded double-layered finlines in which the ferrite layer is transversely magnetized in the substrate plane. The analytical procedure is based on Galerkin's method applied in the Fourier transform domain. This full-wave method is well established and has been successful in the analysis of a wide variety of waveguide structures for microwave and millimeter-wave circuits [6]. Therefore, the detailed mathematical description will be omitted in the following and only the key steps are illustrated.

II. WAVEGUIDE STRUCTURE AND ANALYTICAL METHOD

The waveguide structure under consideration is shown together with the coordinate system for the analysis in Fig. 1. A nonmagnetic layer of thickness h is sandwiched between conductors and a lossless ferrite layer of thickness d . The direction of propagation coincides with the z axis.

Manuscript received April 3, 1987; revised June 30, 1987. This work was supported in part by the Army Research Office under Contract DAAG29-84-K-0076.

M. Geshiro is with the Department of Electrical Engineering, University of Texas at Austin, Austin, TX 78712, on leave from Ehime University, Ehime, Japan.

T. Itoh is with the Department of Electrical Engineering, University of Texas at Austin, Austin, TX 78712.

IEEE Log Number 8717244.

When an external dc magnetic field is applied in the x direction, the tensor permeability of ferrite is expressed as

$$\hat{\mu} = \mu_0 \begin{bmatrix} 1 & 0 & 0 \\ 0 & \mu_r & -jk \\ 0 & jk & \mu_r \end{bmatrix} \quad (1)$$

with

$$\begin{cases} \mu_r = 1 - \frac{\gamma^2 H_0 4\pi M_s}{\omega^2 - (\gamma H_0)^2} \\ \kappa = \frac{\gamma 4\pi M_s \omega}{\omega^2 - (\gamma H_0)^2} \end{cases} \quad (2)$$

where μ_0 , ω , H_0 , $4\pi M_s$, and γ are the free-space permeability, the operating frequency, the applied dc magnetic field, the magnetization of the ferrite, and the gyromagnetic ratio, respectively.

The wave equations for the field components \tilde{E}_x and \tilde{H}_x in the ferrite layer with the permeability tensor given by (1) are derived from Maxwell's equations as

$$\begin{cases} \frac{\partial^2}{\partial y^2} \tilde{E}_x - (\beta^2 + \alpha_n^2 - k_2^2 \mu_e) \tilde{E}_x = -j\omega \mu_0 \xi \alpha_n \tilde{H}_x \\ \frac{\partial^2}{\partial y^2} \tilde{H}_x - \left(\beta^2 + \frac{1}{\mu_r} \alpha_n^2 - k_2^2 \right) \tilde{H}_x = j\omega \epsilon_2 \xi \alpha_n \tilde{E}_x \end{cases} \quad (3)$$

where

$$k_2^2 = \omega^2 \epsilon_2 \mu_0 \quad (4)$$

$$\mu_e = \mu_r - \frac{\kappa^2}{\mu_r} \quad (5)$$

$$\xi = \frac{\kappa}{\mu_r} \quad (6)$$

\tilde{E}_x and \tilde{H}_x are the Fourier transforms of E_x and H_x . For instance,

$$\tilde{E}_x(\alpha_n, y) = \int_{-b}^b E_x(x, y) e^{j\alpha_n x} dx \quad (7)$$

where

$$\alpha_n = \begin{cases} 2\pi n/2b, & n = 0, 1, 2, \dots \text{ for } E_z \text{ odd mode} \\ (2n-1)\pi/2b, & n = 1, 2, 3, \dots \text{ for } E_z \text{ even mode.} \end{cases} \quad (8)$$

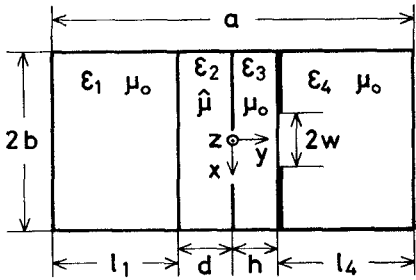


Fig. 1 Cross-sectional view of the ferrite-loaded double-layered finline.

The propagation factor $e^{j(\omega t - \beta z)}$ has been omitted. The solution for (3) can be composed of four elementary waves as

$$\begin{cases} \tilde{E}_x = E^+ e^{-\gamma_+ y} + E^- e^{\gamma_+ y} - Z(H^+ e^{-\gamma_- y} + H^- e^{\gamma_- y}) \\ \tilde{H}_x = -Y(E^+ e^{-\gamma_+ y} + E^- e^{\gamma_+ y}) + H^+ e^{-\gamma_- y} + H^- e^{\gamma_- y} \end{cases} \quad (9)$$

where E^\pm and H^\pm are unknown amplitude coefficients and

$$Z = \frac{\omega \mu_0 \xi \alpha_n}{\gamma_+^2 - (\beta^2 + \alpha_n^2 - k_2^2 \mu_e)} \quad (10)$$

$$Y = \frac{\omega \epsilon_2 \xi \alpha_n}{\gamma_+^2 - \left(\beta^2 + \frac{1}{\mu_r} \alpha_n^2 - k_2^2\right)} \quad (11)$$

$$\gamma_\pm^2 = \beta^2 + \frac{\alpha_n^2}{2} \left(1 + \frac{1}{\mu_r}\right) - \frac{k_2^2}{2} (1 + \mu_e) \pm \sqrt{\left[\frac{\alpha_n^2}{2} \left(1 - \frac{1}{\mu_r}\right) + \frac{k_2^2}{2} (1 - \mu_e)\right]^2 + k_2^2 \xi^2 \alpha_n^2}. \quad (12)$$

The remaining tangential field components \tilde{E}_z and \tilde{H}_z are obtained by

$$\begin{aligned} & \left[(\alpha_n^2 - k_2^2 \mu_r)^2 - (k_2^2 \kappa)^2 \right] \tilde{E}_z \\ &= \alpha_n \beta (\alpha_n^2 - k_2^2 \mu_r) \tilde{E}_x - k_2^2 \kappa \alpha_n \frac{\partial}{\partial y} \tilde{E}_x \\ &+ j \omega \mu_0 \beta \kappa \alpha_n^2 \tilde{H}_x \\ & - j \omega \mu_0 [\mu_r (\alpha_n^2 - k_2^2 \mu_r) + k_2^2 \kappa^2] \frac{\partial}{\partial y} \tilde{H}_x \end{aligned} \quad (13)$$

$$\begin{aligned} & \left[(\alpha_n^2 - k_2^2 \mu_r)^2 - (k_2^2 \kappa)^2 \right] \tilde{H}_z \\ &= \alpha_n \beta (\alpha_n^2 - k_2^2 \mu_r) \tilde{H}_x - k_2^2 \kappa \alpha_n \frac{\partial}{\partial y} \tilde{H}_x \\ & - j \omega \epsilon_2 \beta \kappa k_2^2 \tilde{E}_x + j \omega \epsilon_2 (\alpha_n^2 - k_2^2 \mu_r) \frac{\partial}{\partial y} \tilde{E}_x. \end{aligned} \quad (14)$$

For $\kappa = 0$ and $\mu_r = 1$, the wave equations (3) are reduced to those in the air region or the dielectric layer as

$$\frac{\partial^2}{\partial y^2} \begin{Bmatrix} \tilde{E}_x \\ \tilde{H}_x \end{Bmatrix} - (\beta^2 + \alpha_n^2 - k_i^2) \begin{Bmatrix} \tilde{E}_x \\ \tilde{H}_x \end{Bmatrix} = 0 \quad (15)$$

$$k_i^2 = \omega^2 \epsilon_i \mu_0 \quad i = 1, 3, 4 \quad (16)$$

where \tilde{E}_x and \tilde{H}_x are decoupled. The solutions for those regions are expressed as

$$\begin{cases} \tilde{E}_x = A e^{\gamma_1 (y+d)} \\ \tilde{H}_x = B e^{\gamma_1 (y+d)} \end{cases} \quad y < -d \quad (17)$$

$$\begin{cases} \tilde{E}_x = C \sinh \gamma_3 y + D \cosh \gamma_3 y \\ \tilde{H}_x = F \cosh \gamma_3 y + G \sinh \gamma_3 y \end{cases} \quad 0 < y < h \quad (18)$$

and

$$\begin{cases} \tilde{E}_x = H e^{-\gamma_4 (y-h)} \\ \tilde{H}_x = K e^{-\gamma_4 (y-h)} \end{cases} \quad h < y \quad (19)$$

where

$$\gamma_i^2 = \beta^2 + \alpha_n^2 - k_i^2, \quad i = 1, 3, 4. \quad (20)$$

Eliminating all unknown amplitude coefficients by applying the boundary conditions, we obtain

$$\begin{bmatrix} Y_{xx} & Y_{xz} \\ Y_{zx} & Y_{zz} \end{bmatrix} \begin{bmatrix} \tilde{E}_x \\ \tilde{E}_z \end{bmatrix} = \begin{bmatrix} \tilde{J}_x \\ \tilde{J}_z \end{bmatrix} \quad (21)$$

where \tilde{J}_x and \tilde{J}_z are the Fourier transforms of the current components on the conductors. The matrix elements are known functions of β and α_n , and are given in the Appendix.

Galerkin's procedure is applied in the next step in order to obtain the determinantal equation for the propagation constant. \tilde{E}_x and \tilde{E}_z are expanded in terms of basis functions as

$$\begin{cases} \tilde{E}_x = \sum_{i=1}^M c_i \tilde{\xi}_i(\alpha_n) \\ \tilde{E}_z = \sum_{j=1}^N d_j \tilde{\eta}_j(\alpha_n) \end{cases} \quad (22)$$

where c_i and d_j are unknown coefficients. The basis functions $\tilde{\xi}_i$ and $\tilde{\eta}_j$ should be the Fourier transforms of appropriately chosen functions, which are, in the present paper,

$$\begin{cases} \tilde{\xi}_i(x) = \frac{\cos((i-1)\pi \left(\frac{x}{w} + 1\right))}{\sqrt{1 - \left(\frac{x}{w}\right)^2}} \\ \tilde{\eta}_j(x) = \frac{\sin(j\pi \left(\frac{x}{w} + 1\right))}{\sqrt{1 - \left(\frac{x}{w}\right)^2}}. \end{cases} \quad (23)$$

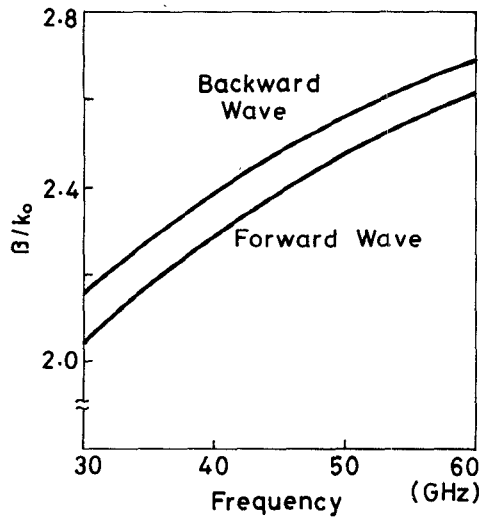


Fig. 2. Dispersion characteristics of the dominant mode propagating in the positive and negative z directions. $\epsilon_{1r} = \epsilon_{4r} = 1$, $\epsilon_{2r} = \epsilon_{3r} = 12.5$, $4\pi M_s = 5000$ G, $H_0 = 500$ Oe, $a = 4b = 4.7$ mm, $l_1 = l_4 = 2.1$ mm, $h = d = 0.25$ mm, $w = 0.5$ mm.

Substitution of (22) into (21), formation of the inner products of the resulting equations with $\tilde{\xi}_i$ and $\tilde{\eta}_j$, and the application of Parseval's relation lead to a homogeneous system of equations for the unknown c_i and d_j :

$$\begin{cases} \sum_{i=1}^M K_{pi}^{xx} c_i + \sum_{j=1}^N K_{pj}^{xz} d_j = 0, & p = 1, 2, \dots, M \\ \sum_{i=1}^M K_{qi}^{zx} c_i + \sum_{j=1}^N K_{qj}^{zz} d_j = 0, & q = 1, 2, \dots, N \end{cases} \quad (24)$$

where

$$\begin{cases} K_{pi}^{xx} = \sum_{n=0}^{\infty} \tilde{\xi}_p(\alpha_n) Y_{xx}(\beta, \alpha_n) \tilde{\xi}_i(\alpha_n) \\ K_{pj}^{xz} = \sum_{n=0}^{\infty} \tilde{\xi}_p(\alpha_n) Y_{xz}(\beta, \alpha_n) \tilde{\eta}_j(\alpha_n) \\ K_{qi}^{zx} = \sum_{n=0}^{\infty} \tilde{\eta}_q(\alpha_n) Y_{zx}(\beta, \alpha_n) \tilde{\xi}_i(\alpha_n) \\ K_{qj}^{zz} = \sum_{n=0}^{\infty} \tilde{\eta}_q(\alpha_n) Y_{zz}(\beta, \alpha_n) \tilde{\eta}_j(\alpha_n). \end{cases} \quad (25)$$

The solution which makes the system determinant associated with (24) equal to zero is the desired propagation constant of the eigenmode. The summation in (25) should be truncated in the numerical computation. For the present analysis, 200 spectral terms are sufficient in each summation.

III. NUMERICAL RESULTS

The accuracy of our solutions, for single-layered structures, has been checked and verified. Our solutions for the dominant mode have overlapped completely with the dispersion curve for the SL_0 mode in [2, fig. 5] throughout the frequency region from 3.2 GHz to 7 GHz. Fig. 2 shows the dispersion characteristics of the dominant

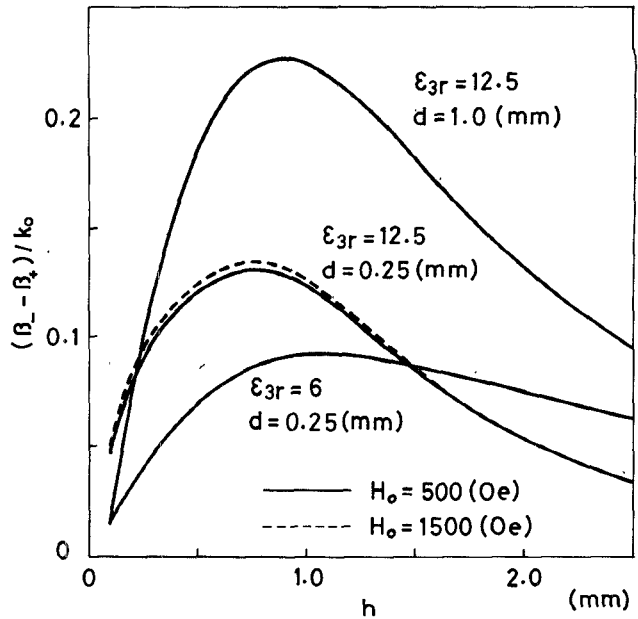


Fig. 3. Differential phase shift versus thickness h of the dielectric layer, $\epsilon_{1r} = \epsilon_{4r} = 1$, $\epsilon_{2r} = 12.5$, $4\pi M_s = 5000$ G, $4b = 4.7$ mm, $w = 0.5$ mm, $f = 45$ GHz.

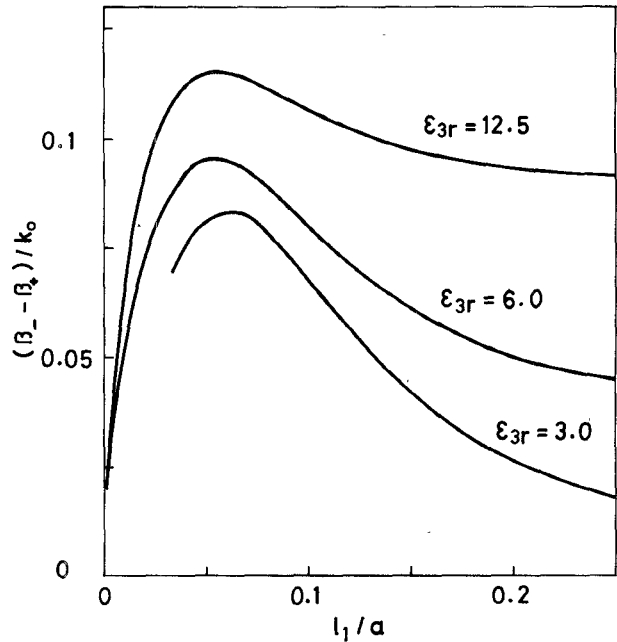


Fig. 4. Differential phase shift versus distance l_1/a from the shielding wall to the ferrite substate. $\epsilon_{1r} = \epsilon_{4r} = 1$, $\epsilon_{2r} = 12.5$, $4\pi M_s = 5000$ G, $H_0 = 500$ Oe, $a = 4b = 4.7$ mm, $h = d = 0.25$ mm, $w = 0.5$ mm, $f = 45$ GHz.

mode propagating in the positive and negative z directions. The first two terms for \tilde{E}_x and one for \tilde{E}_z in (22) are included in the numerical calculations, and are found sufficient to obtain accurate solutions to four significant digits. With the introduction of a dielectric layer, a fairly large nonreciprocity has been achieved (see [5, fig. 3]).

The differential phase shift between the counterpropagating modes is shown in Fig. 3 as a function of thickness d of the dielectric spacer. In this case, the top and bottom conductors of the waveguide shield are removed in order

to eliminate the effects on the propagation characteristics due to varying distance l_1 from the shielding wall to the back surface of the ferrite substrate. The nonreciprocity does not seem to depend drastically on the intensity of the external magnetic field. This is because the resonance frequency is far below the operating frequency for these examples. Note that every curve reaches its peak at a certain value of h .

Finally, Fig. 4 shows curves for the differential phase shifts as a function of finline location in the waveguide shield. There exists a maximum value, as indicated in the literature [1]. It is worthwhile to note that every curve takes its peak at approximately the same value of l_1/a (≈ 0.06) and that they do not seem to depend strongly on the dielectric constant of the spacer. The curve for the case where $\epsilon_{3r} = 3$ is truncated at $l_1/a \approx 0.03$ because one or both of the counterpropagating modes are cut off in the region below this value of l_1/a .

IV. CONCLUSIONS

Nonreciprocal propagations in magnetized-ferrite-loaded double-layered finlines are analyzed based on Galerkin's method in the spectral domain. A number of numerical examples are presented for the propagation constants of the counterpropagating dominant modes. It is confirmed that the dielectric layer introduced between the fin and the ferrite layer can improve the nonreciprocal phase shift characteristics. It is also confirmed that an optimum condition exists for the parameters of the dielectric layer and the finline location in the waveguide shield.

APPENDIX

ELEMENTS OF THE ADMITTANCE MATRIX

$$\begin{bmatrix} Y_{xx} \\ Y_{xz} \end{bmatrix} = \frac{\coth \gamma_4 (l_4 - h)}{t_4} \left\{ -j\hat{\gamma}_4 \begin{bmatrix} 1 \\ 0 \end{bmatrix} + \frac{\alpha_n \beta}{j\hat{\gamma}_4} \begin{bmatrix} -\alpha_n \beta \\ t_4 \end{bmatrix} \right\}$$

$$- \frac{j\hat{\gamma}_3 \gamma_3}{t_3} \left\{ \begin{bmatrix} C_x \\ C_z \end{bmatrix} \cosh \gamma_3 h + \begin{bmatrix} D_x \\ D_z \end{bmatrix} \sinh \gamma_3 h \right\}$$

$$- \frac{\alpha_n \beta}{t_3} \left\{ \begin{bmatrix} F_x \\ F_z \end{bmatrix} \cosh \gamma_3 h + \begin{bmatrix} G_x \\ G_z \end{bmatrix} \sinh \gamma_3 h \right\}$$

$$\begin{bmatrix} Y_{zx} \\ Y_{zz} \end{bmatrix} = \begin{bmatrix} \alpha_n \beta \\ -t_4 \end{bmatrix} \coth \gamma_4 (l_4 - h)$$

$$+ \begin{bmatrix} F_x \\ F_z \end{bmatrix} \cosh \gamma_3 h + \begin{bmatrix} G_x \\ G_z \end{bmatrix} \sinh \gamma_3 h$$

$$[C_x, C_z] = \left[\left\{ \frac{1}{\sinh \gamma_3 h} - \frac{\coth \gamma_3 h}{\Delta_3} (j\hat{\gamma}_3 \gamma_3 C_{22} - \alpha_n \beta C_{12}) \right\}, \frac{t_3 C_{12}}{\Delta_3} \coth \gamma_3 h \right]$$

$$[D_x, D_z] = [(j\hat{\gamma}_3 \gamma_3 C_{22} - \alpha_n \beta C_{12})/\Delta_3, t_3 C_{12}/\Delta_3]$$

$$[F_x, F_z] = [(\alpha_n \beta C_{11} - j\hat{\gamma}_3 \gamma_3 C_{21})/\Delta_3, -t_3 C_{11}/\Delta_3]$$

$$[G_x, G_z] = \left[\left\{ \frac{\alpha_n \beta}{j\hat{\gamma}_3 \sinh \gamma_3 h} - \frac{\tanh \gamma_3 h}{\Delta_3} \right. \right.$$

$$\times (\alpha_n \beta C_{11} - j\hat{\gamma}_3 \gamma_3 C_{21}) \Big\},$$

$$\left. \left. \times \left\{ \frac{t_3}{j\hat{\gamma}_3 \cosh \gamma_3 h} + \frac{\tanh \gamma_3 h}{\Delta_3} t_3 C_{11} \right\} \right\} \right]$$

$$\Delta_3 = C_{11} C_{22} - C_{12} C_{21}$$

$$C_{11} = j\hat{\gamma}_3 \gamma_3 \cosh \gamma_3 h + \xi_{21} \sinh \gamma_3 h$$

$$C_{12} = (-\alpha_n \beta + \xi_{22}) \sinh \gamma_3 h$$

$$C_{21} = (\alpha_n \beta - \xi_{11}) \cosh \gamma_3 h$$

$$C_{22} = j\hat{\gamma}_3 \sinh \gamma_3 h - \xi_{12} \cosh \gamma_3 h$$

$$\xi_{1i} = t_3 \{ a_{1i} (P_+ + jy_1^+ Q_+ - jy_2^+ Q_-) + a_{2i} (P_- + jy_1^- Q_+ - jy_2^- Q_-) \}$$

$$\xi_{2i} = t_3 \{ a_{1i} (jR_+ + y_1^+ S_+ - y_2^+ S_-) + a_{2i} (jR_- + y_1^- S_+ - y_2^- S_-) \}, \quad i=1,2$$

$$a_{11} = \{ jY + (y_1^- - y_2^-) \} / \Delta_2$$

$$a_{12} = -\{ 1 - jZ(y_1^- - y_2^-) \} / \Delta_2$$

$$a_{21} = -\{ jY + (y_1^+ - y_2^+) \} / \Delta_2$$

$$a_{22} = \{ 1 - jZ(y_1^+ - y_2^+) \} / \Delta_2$$

$$\Delta_2 = \{ 1 - jZ(y_1^+ - y_2^+) \} \{ jY + (y_1^- - y_2^-) \} - \{ 1 - jZ(y_1^- - y_2^-) \} \{ jY + (y_1^+ - y_2^+) \}$$

$$y_1^\pm = \exp [(\pm \gamma_+ - \gamma_-) d] \cdot \{ (-d_1 + t_1 S_-) (a_1 - t_1 P_\pm) + (b_1 + t_1 Q_-) (c_1 - t_1 R_\pm) \} / \Delta_1$$

$$y_2^\pm = \exp [(\pm \gamma_+ + \gamma_-) d] \cdot \{ (-d_1 + t_1 S_+) (a_1 - t_1 P_\pm) + (b_1 + t_1 Q_+) (c_1 - t_1 R_\pm) \} / \Delta_1$$

$$\Delta_1 = j t_1 \{ t_1 (Q_+ S_- - Q_- S_+) - b_1 (S_+ - S_-) - d_1 (Q_+ - Q_-) \}$$

$$\begin{bmatrix} a_1 & b_1 \\ c_1 & d_1 \end{bmatrix} = \alpha_n \beta \begin{bmatrix} 1 & Z \\ Y & 1 \end{bmatrix} + \gamma_1 \begin{bmatrix} \hat{z} Y \tanh \gamma_1 (l_1 - d), \hat{z} \tanh \gamma_1 (l_1 - d) \\ \hat{y}_1 \coth \gamma_1 (l_1 - d), \hat{y}_1 Z \coth \gamma_1 (l_1 - d) \end{bmatrix}$$

$$\hat{z} = \omega \mu_0, \quad \hat{y}_i = \omega \epsilon_i, \quad t_i = \alpha_n^2 - k_i^2, \quad i=1,2,3,4$$

$$P_\pm = \beta (\alpha_n p - \hat{z} \kappa \nu Y) \pm \gamma_\pm (\alpha_n s - \hat{z} u Y)$$

$$R_\pm = \beta (\alpha_n p Y - \hat{y}_2 s) \pm \gamma_+ (\alpha_n s Y - \hat{y}_2 p)$$

$$Q_\pm = \beta (-\alpha_n p Z + \hat{z} \kappa \nu) \pm \gamma_- (-\alpha_n s Z + \hat{z} u)$$

$$S_\pm = \beta (\alpha_n p - \hat{y}_2 s Z) \pm \gamma_- (\alpha_n s - \hat{y}_2 p Z)$$

$$p = (\alpha_n^2 - k_2^2 \mu) / q, \quad s = k_2^2 \kappa / q,$$

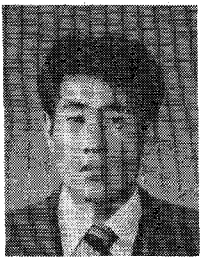
$$u = \{ \mu (\alpha_n^2 - k_2^2 \mu) + k_2^2 \kappa^2 \} / q$$

$$\nu = \alpha_n^2 / q, \quad q = (\alpha_n^2 - k_2^2 \mu)^2 - (k_2^2 \kappa)^2.$$

REFERENCES

- [1] A. Beyer and K. Solback, "A new fin-line ferrite isolator for integrated millimeter-wave circuits," *IEEE Trans. Microwave Theory Tech.*, vol. MTT-29, pp. 1344-1348, Dec. 1981.
- [2] F. J. K. Lange, "Analysis of shielded strip- and slot-lines on a ferrite substrate transversely magnetized in the plane of the substrate," *Arch. Elek. Übertragung*, vol. 36, no. 3, pp. 95-100, Mar. 1982.
- [3] G. Bock, "Dispersion characteristics of slot line on a ferrite substrate by a mode-matching technique," *Electron. Lett.*, vol. 18, no. 12, pp. 536-537, Mar. 1982.
- [4] J. Mazur and K. Grabowski, "Spectral domain analysis of multilayered transmission lines with anisotropic media," presented at URSI Symp. on EMW, Munich, 1980.
- [5] Y. Hayashi and R. Mittra, "An analytical investigation of finlines with magnetized ferrite substrate," *IEEE Trans. Microwave Theory Tech.*, vol. MTT-31, pp. 495-498, June 1983.
- [6] T. Itoh and R. Mittra, "Spectral-domain approach for calculating the dispersion characteristics of microstrip lines," *IEEE Trans. Microwave Theory Tech.*, vol. MTT-21, pp. 496-499, July 1973.

*



Masahiro Geshiro (S'75-M'78) received the B.E., M.E., and Ph.D. degrees in 1973, 1975, and 1978, respectively, from Osaka University, Osaka, Japan.

In December 1979 he joined the Department of Electronics, Ehime University, Matsuyama, Japan, where he is now an Associate Professor of Electronics Engineering. From March 1986 to January 1987, he was a Visiting Scholar at the University of Texas at Austin, on leave from Ehime University. He has been engaged in re-

search on optical transmission lines and optical integrated circuits.

Dr. Geshiro is a member of the Institute of Electronics, Information, and Communication Engineers of Japan.

*



Tatsuo Itoh (S'69-M'69-SM'74-F'82) received the Ph.D. degree in electrical engineering from the University of Illinois, Urbana, in 1969.

From September 1966 to April 1976, he was with the Electrical Engineering Department, University of Illinois. From April 1976 to August 1977, he was a Senior Research Engineer in the Radio Physics Laboratory, SRI International, Menlo Park, CA. From August 1977 to June 1978, he was an Associate Professor at the University of Kentucky, Lexington. In July 1978, he

joined the faculty at the University of Texas at Austin, where he is now a Professor of Electrical and Computer Engineering and Director of the Electrical Engineering Research Laboratory. During the summer of 1979, he was a guest researcher at AEG-Telefunken, Ulm, West Germany. Since September 1983, he has held the Hayden Head Centennial Professorship of Engineering at the University of Texas. In September 1984, he was appointed Associate Chairman for Research and Planning of the Electrical and Computer Engineering Department.

Dr. Itoh is a member of the Institute of Electronics and Communication Engineers of Japan, Sigma Xi, and Commissions B and D of USNC/URSI. He served as the Editor of the *IEEE TRANSACTIONS ON MICROWAVE THEORY AND TECHNIQUES* for 1983-1985. He serves on the Administrative Committee of the IEEE Microwave Theory and Techniques Society. Dr. Itoh is a Professional Engineer registered in the state of Texas.